


Relevance of Shear Transformations in the Relaxation of Supercooled Liquids

Matthias Lerbinger,^{*} Armand Barbot, Damien Vandembroucq[✉], and Sylvain Patinet[†]
PMMH, CNRS, ESPCI Paris, Université PSL, Sorbonne Université, Université Paris Cité, 75005 Paris, France

 (Received 25 September 2021; revised 18 July 2022; accepted 9 October 2022; published 31 October 2022)

While deeply supercooled liquids exhibit divergent viscosity and increasingly heterogeneous dynamics as the temperature drops, their structure shows only seemingly marginal changes. Understanding the nature of relaxation processes in this dramatic slowdown is key for understanding the glass transition. Here, we show by atomistic simulations that the heterogeneous dynamics of glass-forming liquids strongly correlate with the local residual plastic strengths along soft directions computed in the initial inherent structures. The correlation increases with decreasing temperature and is maximum in the vicinity of the relaxation time. For the lowest temperature investigated, this maximum is comparable with the best values from the literature dealing with the structure-property relationship. However, the nonlinear probe of the local shear resistance in soft directions provides here a real-space picture of relaxation processes. Our detection method of thermal rearrangements allows us to investigate the first passage time statistics and to study the scaling between the activation energy barriers and the residual plastic strengths. These results shed new light on the nature of relaxations of glassy systems by emphasizing the analogy between the thermal relaxations in viscous liquids and the plastic shear transformation in amorphous solids.

DOI: [10.1103/PhysRevLett.129.195501](https://doi.org/10.1103/PhysRevLett.129.195501)

When cooled fast enough, most substances avoid crystallization and form a glass [1]. Before reaching the glass transition, they are trapped in a supercooled liquid metastable state, with a diverging relaxation time as the temperature is lowered, and show complex dynamics [2] marked by the presence of dynamical heterogeneities [3]. A fundamental problem in condensed matter that has remained unsolved so far is that it is extremely difficult to identify any structural signature associated with this dramatic change in dynamics. Still, a clear link between structure and dynamics is implied by the increased sensitivity of the dynamics to the initial structural conditions as the temperature decreases [4]. Recent major advances rely on the identification of the so-called locally favored structures [5] and indicate the necessity of employing a locally coarse-grained description of the structure [6–8]. Remarkable progress has also been achieved using multibody order parameters [9,10] or advanced machine learning methods [11–15].

Although these different approaches have established an unprecedented link between local dynamics and structure, most rely upon scalar quantities, i.e., they disregard the orientation dependencies. Furthermore, the underlying mechanisms of the relaxation processes have remained elusive. Contrasting results have been reported in the literature showing that thermally activated excitations could take the form of single atomic jumps [16], stringlike motions [17–19], or local shears [20]. In all cases, the spatial structure of the relaxations tends to localize with decreasing temperature [21,22].

A promising approach to understanding the relaxation of supercooled liquids consists of reversing the problem by

considering highly viscous liquids as flowing solids [23]. The rationale behind this approach relies upon the description of liquids from a potential energy landscape point of view [24,25]. In this picture, for sufficiently low temperatures, the system spends most of its time vibrating around potential energy minima before quickly jumping to other minima. A succession of Inherent States (ISs) can thus describe the dynamics [26]. More than a mere simplification, this solidlike description has enabled the understanding of key aspects of glass-forming liquids from a mechanical description of their ISs [27,28]. Perturbative approaches based on soft vibrational modes have been linked to irreversible rearrangements [29], a non-Arrhenian characteristic energy scale has been identified in fragile liquids [30,31], and the presence of long-range anisotropic stress correlations explained [32]. All of these studies point to the importance of soft localized excitations. However, a direct link between relaxations in liquids and the local nonlinear plastic rearrangements of ISs remains to be established [33].

This Letter aims to demonstrate how local soft directions in the initial ISs account for the local relaxation rates of the parent supercooled liquids. For this, we rely on a local shear test (LST) numerical method providing access to the local residual plastic strength $\Delta\tau^c$ [34]. This structural indicator has proved to be very helpful in athermal amorphous solids for capturing the barrier dependencies to preparation [35], shear banding [36], anisotropy [37], and to predict plastic activity [38].

We analyze molecular dynamics (MD) simulations of supercooled liquids equilibrated at different temperatures

from which temporal series of ISs are generated. A strong connection is established between the local residual plastic strength computed in the initial ISs along the weakest shear direction and the local dynamics. The maximum correlation is found around the system relaxation time t_α and increases as the temperature decreases. Additionally, a remarkable correlation is established between the core displacement fields of athermal plastic and thermal rearrangements, respectively observed in LST and MD. The thermal excitations are shown to be more frequent in the softest shear directions, thus providing a real-space picture of the relaxation processes. Local relaxation locations and first passage times are detected using the linear response of underlying ISs. This method allows us to investigate the scaling relation between the energy barriers and the residual plastic strengths [39–41].

Simulation methods.—The systems under study are two-dimensional binary mixtures [35]. A sample contains 10^4 atoms interacting via Lennard-Jones (LJ) potentials vanishing at a cutoff distance $R_{\text{cut}} = 2.5$ (see the Supplemental Material [42]). MD simulations are performed in the *NVT* ensemble in square boxes equipped with periodic boundary conditions. In the following, all observables are expressed in LJ units.

The results that we analyze are taken from 20 independent samples simulated at three temperatures $T = 0.5$, 0.351, and 0.32, respectively located around the onset temperature, the mode-coupling crossover and in a regime below which the MD equilibrium sampling starts to be numerically untractable. The systems are equilibrated such that the potential energy is stationary over a time $100t_\alpha$. The relaxation time t_α is estimated from the self-intermediate scattering function $F_{s,\text{CR}}(q, t)$ using the first neighbor cage-relative (CR) displacements $\Delta\vec{r}_{\text{CR}}$ [45] such that $F_{s,\text{CR}}(q = 2\pi/a, t = t_\alpha) = 1/e$, with a the average atomic distance. Going from high to low temperature, the relaxation time diverges: $t_\alpha = 7, 243, \text{ and } 10999$.

ISs are generated along the MD run by instantaneously quenching configurations at logarithmic increasing time intervals [see Fig. 1(a)]. MD configurations are relaxed with balanced forces on each atom using a conjugate gradient algorithm. The kinematics of supercooled liquids can then be greatly simplified and reduced to a sequence of ISs by removing thermal vibrations. Studying the inherent dynamics allows us to focus on the influence of the underlying potential energy landscape [18,26,27].

In Figs. 1(b) and 1(c), we respectively show typical core and long-range thermal rearrangement displacement fields \vec{u}_{th} between two ISs. We observe a strong localization of \vec{u}_{th} around rearrangements. The displacement fields in the core of these localized excitations show a wide range of complex behaviors, from single atomic jumps to more spread and intricate patterns. However, a striking feature of the long-range \vec{u}_{th} is the presence of quadrupolar symmetries [32,46] around the rearrangements as shown in Fig. 1(c). This is a characteristic feature of Eshelby’s plastic

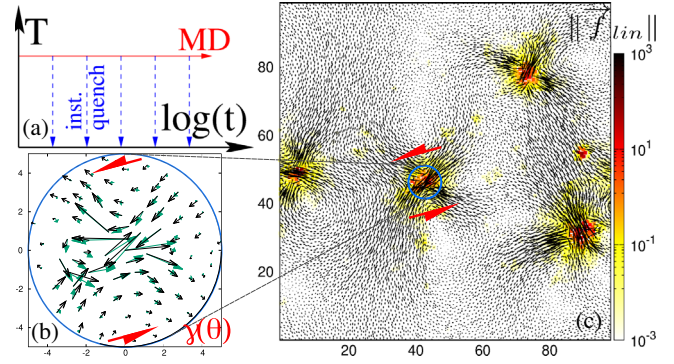


FIG. 1. Methods: (a) Generation of ISs by instantaneous quench from MD trajectories. $\Delta\tau^c(\vec{r}, \theta)$ are sampled in the initial ISs at $t = 0$. (b) Normalized thermal rearrangement core displacement field \vec{u}_{th} (black arrows) between two ISs separated by $\Delta t = 0.1$ from a liquid at $T = 0.32$. The corresponding normalized LST displacement field \vec{u}_{LST} (cyan arrows) that maximizes the correlation over θ is found in the vicinity of the softest direction. (c) Corresponding far displacement (arrows) and linear response $\|\vec{f}_{\text{lin}}\|$ (colors) fields.

shear transformations, more commonly discussed in the context of amorphous plasticity [47,48]. This is a strong hint of the local shear character of thermally activated events in supercooled liquids [20]. We also observe exchange events between atoms, without long-range elastic response, that remain in the minority [42].

Local shear test method.—To study the influence of mechanical properties of the initial structure on the dynamics, we perform LSTs [35] in the ISs at time $t = 0$. The method consists of shearing a local circular inclusion at position \vec{r} by applying affine pure shear boundary conditions to the surrounding atoms in a shear direction θ (see Fig. 1). The atoms inside are deformed via the quasistatic athermal method [49] and can relax nonaffinely. The inclusion is loaded until a drop in local stress indicates the first plastic instability [42]. We extract two quantities from the LSTs: the residual plastic strength $\Delta\tau^c(\vec{r}, \theta)$ and the plastic instability displacement field corresponding to the stress drop $\vec{u}_{\text{LST}}(\vec{r}, \theta)$. These two observables are sampled with inclusion radii $R_{\text{free}} = 5$, at positions \vec{r} on a regular square grid of lattice parameter R_{cut} and in 18 directions θ , every $\Delta\theta = 10^\circ$.

The values of $\Delta\tau^c$ statistically increase when decreasing the parent temperature [42], showing that this observable is able to capture the energy barrier’s increase with the decrease of the temperature, i.e., the liquid fragility [1,50]. In the following, we show that $\Delta\tau^c$ also determines most of the spatial fluctuations of the dynamics. While isotropy prevails in a statistical sense, the values of the directional $\Delta\tau^c(\vec{r}, \theta)$ strongly depend on the local shear directions and positions, thus reflecting the disordered character of the amorphous structure [35,37]. For liquids, the thermally induced excitations are statistically isotropic, so one would expect the onset of local relaxations to be

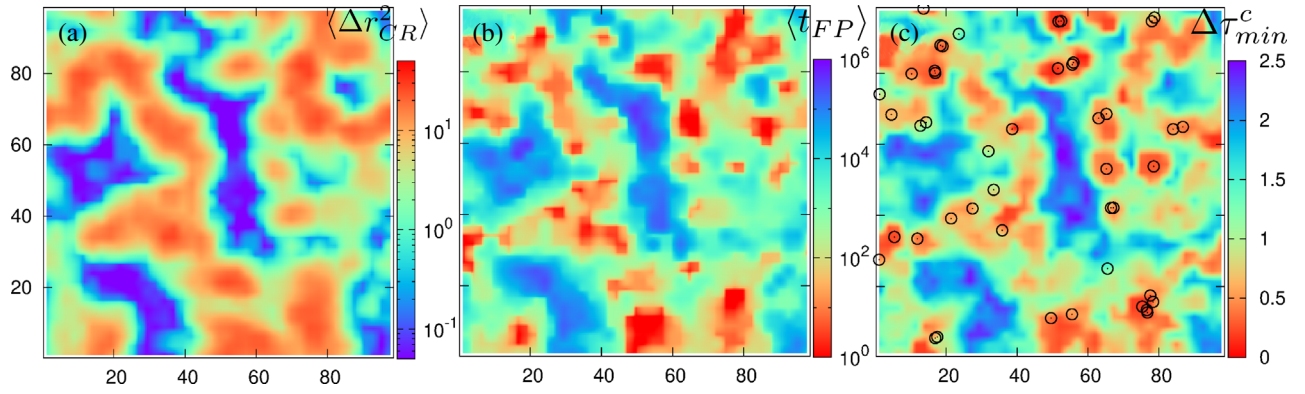


FIG. 2. Dynamical propensity $\langle \Delta r_{CR}^2(t=t_\alpha) \rangle$ (a), average first passage time $\langle t_{FP} \rangle$ (b), and residual plastic strength in the softest direction $\Delta \tau_{min}^c$ (c) at $T = 0.32$. The open circles correspond to the location of the first 50 isolated thermal rearrangements.

dominated by the residual strengths along the weakest directions: $\Delta \tau_{min}^c(\vec{r}) = \min_\theta \Delta \tau^c(\vec{r}, \theta)$. We therefore consider in the following these values in local softest directions $\theta_{min}(\vec{r})$ and compare them with the system dynamics.

Dynamical observables.—To emphasize the influence of the structure, we perform MD simulations in the isoconfigurational ensemble [4]. In this ensemble, multiple independent runs are started using the same initial configuration, but the particles' momenta are drawn from a Maxwell-Boltzmann distribution for each run. For each starting configuration, 100 replica are simulated. The dynamic propensity $\langle \Delta r_{CR}^2(t) \rangle$ is computed as a function of time by averaging the CR square displacement over the isoconfigurational ensemble of each atom [33]. The propensity is finally coarse grained on the same regular grid as $\Delta \tau_{min}^c$ with a coarse-graining length equal to R_{cut} to compare these quantities on an equal footing. A $\langle \Delta r_{CR}^2(t) \rangle$ map is reported in Fig. 2(a). It shows the characteristic dynamical heterogeneities [2,3], with some broadening due to the coarse-graining procedure [42].

Although valuable, the information provided by $\langle \Delta r_{CR}^2(t) \rangle$ results from an accumulation of rearrangements which cannot be analyzed separately. To address this issue, and detect the positions of rearrangements, we compute the linear force response \vec{f}_{lin} between two ISs [32]. From time t_0 to t , $\vec{f}_{lin}(t, t_0) = H_{t_0} \cdot \vec{u}_{th}(t, t_0)$ where H_{t_0} is the Hessian matrix evaluated in the IS at t_0 . We then consider the norm $\|\vec{f}_{lin}\|$ on each atom. If the atom motions correspond to the linear response of the system, $\|\vec{f}_{lin}\|$ is equal to zero because of mechanical balance. On the other hand, large $\|\vec{f}_{lin}\|$ are expected in the highly distorted, nonlinear regions. This is what is observed in Fig. 1(c) where $\|\vec{f}_{lin}\|$ features large values at the cores of the thermal rearrangements while vanishing in the rest of the system. Although it requires working in ISs, several advantages of this method should be stressed. First, it is sensitive and $\|\vec{f}_{lin}\|$ spans several orders of magnitude between rearranged and elastically disturbed regions. Second, it erases the long-range linear elastic fields

induced by rearrangements. Finally, it is not affected by rigid body motions.

We choose to consider as being rearranged the atoms for which $\|\vec{f}_{lin}(t, t_0)\| > f^*$, with $f^* = 7$ [42]. This allows us to define the local first passage time t_{FP} when this criterion is fulfilled for the first time during a trajectory starting from $t_0 = 0$. For each time lag Δt and for each isolated clusters of atoms with $\|\vec{f}_{lin}(\Delta t = t - t_0)\| > f^*$, the locations of the successive isolated thermal rearrangements are extracted from the positions of the atom carrying the largest $\|\vec{f}_{lin}\|$. For each event, we also record the local maximum shear strain direction denoted θ_{th} from the local strain field [36]. The number of events between two ISs increases with temperature and time window Δt . The isoconfigurational averages of first passage times $\langle t_{FP} \rangle$ reported in Fig. 2(b) show again characteristic dynamical heterogeneities of supercooled liquids. The comparison of $\langle \Delta r_{CR}^2(t=t_\alpha) \rangle$ and $\langle t_{FP} \rangle$ shows striking similarities, meaning that parts of the short and long dynamics are correlated. In our view, however, $\langle t_{FP} \rangle$ provides an easier grasp of the initial local structural relaxation timescale compared with accumulated mean square displacements.

Correlation between dynamics and $\Delta \tau_{min}^c$.—In Fig. 2, we compare the $\langle \Delta r_{CR}^2(t=t_\alpha) \rangle$, $\langle t_{FP} \rangle$, and $\Delta \tau_{min}^c$ maps. Their similarity is remarkable. The softer the region, the faster its relaxation. As an example, the first 50 isolated thermal events of a particular MD trajectory are reported in Fig. 2(c). They are systematically located in the softest areas. More quantitatively, to analyze the correlation between the rearrangement locations and the initial structure, we report in Fig. 3(a) the ranking correlation defined in Ref. [34] from the cumulative distribution function F_X as $C(t) = 1 - 2F_X(X, t)$ where $X = \Delta \tau_{min}^c$ is the value of the field at $t = 0$ where the thermal event takes place at t . $C(t)$ shows that the correlation is larger for the smallest temperatures and decreases over time, the system losing the memory of its original structure.

The Pearson correlation ρ between the fields $\Delta \tau_{min}^c(t=0)$ and $\ln[\langle \Delta r_{CR}^2(t) \rangle]$ is plotted as a function of time in Fig. 3(b).

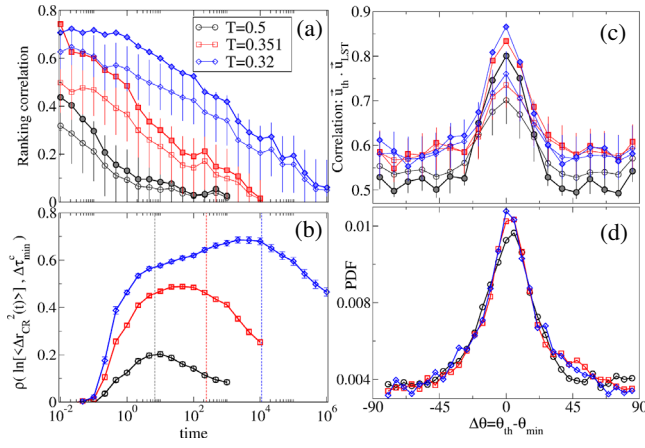


FIG. 3. Correlation between the thermal rearrangements and the initial residual plastic strengths in the weakest directions $\Delta\tau_{\min}^c$. Open and filled symbols correspond to the average and the median, respectively. Ranking (a) and Pearson correlations (b) as a function of time. (c) Correlation between thermal and LST displacement fields [see Fig. 1(b)] as a function of the angular difference $\Delta\theta = \theta_{\text{th}} - \theta_{\text{min}}$ between the shear strain of the thermal rearrangement and the softest direction. (d) $\Delta\theta$ probability distribution function.

We observe that the correlation increases with time as the successive thermal relaxations accumulate, with a peak around t_α . The correlation with the $\langle t_{\text{FP}} \rangle$ field is quantitatively close to that with $\langle \Delta r_{\text{CR}}^2(t = t_\alpha) \rangle$ [42]. Remarkably, for the lowest temperature, we find a maximum correlation $\rho \approx 0.7$ comparable to the maximum correlations found in literature such those obtained from machine learning [12,13] and to the order parameter proposed in Ref. [9] (see the Supplemental Material for a detailed comparison [42]).

We go one step further and directly evaluate the correlation between \vec{u}_{th} and \vec{u}_{LST} in the core regions of the first passage rearrangements. An example of such a comparison reported in Fig. 1(b) shows a striking agreement between the two fields. The correlation is calculated as the maximum over all LST directions θ of the dot product of the normalized vector fields \vec{u}_{th} and \vec{u}_{LST} . Figure 3(c) shows correlation as a function of the orientation deviation $\Delta\theta = \theta_{\text{th}} - \theta_{\text{min}}$. We observe a maximum when the thermal rearrangements are aligned with the softest directions, i.e., for $\Delta\theta = 0$. This maximum of correlation obtained on the full set of first passage thermal rearrangements reaches significantly high values with a median in the range $[0.8 - 0.86]$ while the mean lies a bit below in the range $[0.7 - 0.76]$. This slight contrast reflects the fact that the distribution presents a peak close to 1, i.e., to quasi-identity between plastic and thermal events.

In addition to barrier heights, this result shows that the mechanisms of shear transformation and thermal relaxation share remarkable similarities. Besides the correlation, we report in Fig. 3(d) the $\Delta\theta$ probability distribution showing a clear peak around $\Delta\theta = 0$, which means that thermal rearrangement's shear directions are more frequent in the

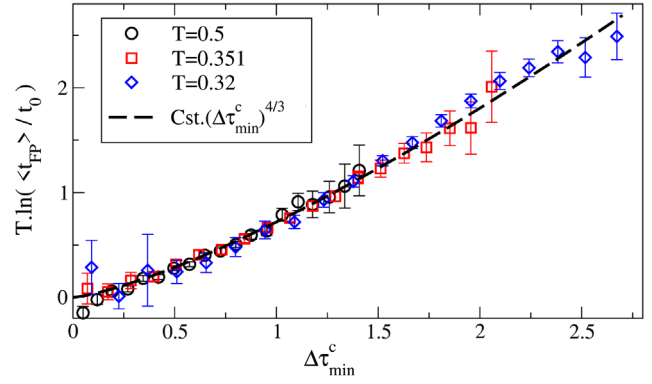


FIG. 4. Energy barrier ΔU estimated from the average first passage time $\langle t_{\text{FP}} \rangle$ as a function of the residual plastic strength $\Delta\tau_{\min}^c$. t_0 is a tunable parameter fitted to collapse the data. The dashed line shows the scaling law found in Ref. [51].

vicinity of softest directions. This last observation is fully consistent with the interpretation of fast dynamics in the soft regions of ISs, whose hop frequencies are dominated by the weakest directions.

Scaling of energy barriers.—Once the correlation is established, we discuss now the quantitative relation between $\langle t_{\text{FP}} \rangle$ and $\Delta\tau_{\min}^c$. The effective activation energy is fitted assuming an Arrhenius law in the form $\langle t_{\text{FP}} \rangle = t_0 e^{\Delta U/T}$ with t_0 a prefactor and ΔU the energy barrier. The actual temperature dependence of the characteristic time t_0 is disregarded, and t_0 is used as a tunable parameter allowing one to collapse the results obtained at different temperatures. As shown in Fig. 4, we find a scaling of barriers as a function of the residual plastic strengths $\Delta U \sim (\Delta\tau_{\min}^c)^\beta$. If an exponent $\beta = 3/2$, compatible with the catastrophe theory [39–41], can not be totally ruled out, the fit of our data gives $\beta = 1.33 \pm 0.03$. Interestingly, this result is in quantitative agreement with $\beta = 4/3$, a scaling that can be deduced from the relations $\Delta U \sim \omega^4$ and $\Delta\tau^c \sim \omega^3$ found in Ref. [51] [see Eqs. (35) and (37) therein] where ω is the frequency of the nonlinear quasilocalized excitations in quiescent glasses. It is to our knowledge the first time it has been obtained locally at finite temperature. This scaling relation can be understood as a reflection of the sensitivity of the lowest barriers to stress, which is identified here in the local softest directions by the LST.

Concluding remarks and perspectives.—In this Letter, we have established a strong correlation between residual plastic strengths in the softest direction of the initial IS and the dynamics of glass-forming liquids. The softer the zones of ISs, the faster the local region of liquids. An advantage of this picture over purely geometrical approaches is that it provides a simple real-space interpretation of relaxations as localized shear events in soft directions. Among the possible transition paths, a local shear allows particles to escape from their cage for moderate long-range elastic energy cost. As a local stress, $\Delta\tau_{\min}^c$ is a naturally coarse-grained quantity [6,7]. Shear transformations thus involve

cooperative motions in the spirit of an Adam-Gibbs-style scenario [1,52] and long-range generated elastic interactions providing intuitive support to the dynamic facilitation picture [53–55]. By pointing to the central role played by the mechanics of ISs at low temperatures, these results are useful for understanding the onset of rigidity and the theoretical description of the glass transition.

*Deceased.

†sylvain.patinet@espci.fr

- [1] A. Cavagna, *Phys. Rep.* **476**, 51 (2009).
- [2] A. S. Keys, L. O. Hedges, J. P. Garrahan, S. C. Glotzer, and D. Chandler, *Phys. Rev. X* **1**, 021013 (2011).
- [3] M. D. Ediger, *Annu. Rev. Phys. Chem.* **51**, 99 (2000).
- [4] A. Widmer-Cooper, P. Harrowell, and H. Fynewever, *Phys. Rev. Lett.* **93**, 135701 (2004).
- [5] A. Malins, J. Eggers, C. P. Royall, S. R. Williams, and H. Tanaka, *J. Chem. Phys.* **138**, 12A535 (2013).
- [6] L. Berthier and R. L. Jack, *Phys. Rev. E* **76**, 041509 (2007).
- [7] H. Tong and H. Tanaka, *Phys. Rev. X* **8**, 011041 (2018).
- [8] E. Boattini, F. Smallenburg, and L. Filion, *Phys. Rev. Lett.* **127**, 088007 (2021).
- [9] H. Tong and H. Tanaka, *Nat. Commun.* **10**, 5596 (2019).
- [10] H. Tong and H. Tanaka, *Phys. Rev. Lett.* **124**, 225501 (2020).
- [11] S. S. Schoenholz, E. D. Cubuk, D. M. Sussman, E. Kaxiras, and A. J. Liu, *Nat. Phys.* **12**, 469 (2016).
- [12] V. Bapst, T. Keck, A. Grabska-Barwińska, C. Donner, E. D. Cubuk, S. S. Schoenholz, A. Obika, A. W. R. Nelson, T. Back, D. Hassabis, and P. Kohli, *Nat. Phys.* **16**, 448 (2020).
- [13] E. Boattini, S. Marín-Aguilar, S. Mitra, G. Foffi, F. Smallenburg, and L. Filion, *Nat. Commun.* **11**, 5479 (2020).
- [14] J. Paret, R. L. Jack, and D. Coslovich, *J. Chem. Phys.* **152**, 144502 (2020).
- [15] M. Sharma, M. K. Nandi, and S. M. Bhattacharyya, *Phys. Rev. E* **105**, 044604 (2022).
- [16] K. Vollmayr-Lee, *J. Chem. Phys.* **121**, 4781 (2004).
- [17] C. Donati, S. C. Glotzer, P. H. Poole, W. Kob, and S. J. Plimpton, *Phys. Rev. E* **60**, 3107 (1999).
- [18] M. Vogel, B. Doliwa, A. Heuer, and S. C. Glotzer, *J. Chem. Phys.* **120**, 4404 (2004).
- [19] W. Ji, T. W. J. de Geus, E. Agoritsas, and M. Wyart, *Phys. Rev. E* **105**, 044601 (2022).
- [20] A. Widmer-Cooper and P. Harrowell, *Phys. Rev. E* **80**, 061501 (2009).
- [21] D. Coslovich, A. Ninarello, and L. Berthier, *SciPost Phys.* **7**, 77 (2019).
- [22] M. Shimada, D. Coslovich, H. Mizuno, and A. Ikeda, *SciPost Phys.* **10**, 001 (2021).
- [23] J. C. Dyre, *Rev. Mod. Phys.* **78**, 953 (2006).
- [24] M. Goldstein, *J. Chem. Phys.* **51**, 3728 (1969).
- [25] P. G. Debenedetti and F. H. Stillinger, *Nature (London)* **410**, 259 (2001).
- [26] B. Doliwa and A. Heuer, *Phys. Rev. Lett.* **91**, 235501 (2003).
- [27] A. Heuer, *J. Phys. Condens. Matter* **20**, 373101 (2008).
- [28] E. Del Gado, P. Ilg, M. Kröger, and H. C. Öttinger, *Phys. Rev. Lett.* **101**, 095501 (2008).
- [29] A. Widmer-Cooper, H. Perry, P. Harrowell, and D. R. Reichman, *Nat. Phys.* **4**, 711 (2008).
- [30] E. Lerner and E. Bouchbinder, *J. Chem. Phys.* **148**, 214502 (2018).
- [31] G. Kapteijns, D. Richard, E. Bouchbinder, T. B. Schrøder, J. C. Dyre, and E. Lerner, *J. Chem. Phys.* **155**, 074502 (2021).
- [32] A. Lemaître, *Phys. Rev. Lett.* **113**, 245702 (2014).
- [33] Y.-W. Li, Y. Yao, and M. P. Ciamarra, *Phys. Rev. Lett.* **128**, 258001 (2022).
- [34] S. Patinet, D. Vandembroucq, and M. L. Falk, *Phys. Rev. Lett.* **117**, 045501 (2016).
- [35] A. Barbot, M. Lerbinger, A. Hernandez-Garcia, R. García-García, M. L. Falk, D. Vandembroucq, and S. Patinet, *Phys. Rev. E* **97**, 033001 (2018).
- [36] A. Barbot, M. Lerbinger, A. Lemaître, D. Vandembroucq, and S. Patinet, *Phys. Rev. E* **101**, 033001 (2020).
- [37] S. Patinet, A. Barbot, M. Lerbinger, D. Vandembroucq, and A. Lemaître, *Phys. Rev. Lett.* **124**, 205503 (2020).
- [38] D. Richard, M. Ozawa, S. Patinet, E. Stanifer, B. Shang, S. A. Ridout, B. Xu, G. Zhang, P. K. Morse, J.-L. Barrat, L. Berthier, M. L. Falk, P. Guan, A. J. Liu, K. Martens, S. Sastry, D. Vandembroucq, E. Lerner, and M. L. Manning, *Phys. Rev. Mater.* **4**, 113609 (2020).
- [39] W. L. Johnson and K. Samwer, *Phys. Rev. Lett.* **95**, 195501 (2005).
- [40] C. E. Maloney and D. J. Lacks, *Phys. Rev. E* **73**, 061106 (2006).
- [41] Y. Fan, T. Iwashita, and T. Egami, *Nat. Commun.* **5**, 5083 (2014).
- [42] See Supplemental Material at <http://link.aps.org/supplemental/10.1103/PhysRevLett.129.195501> for details about the system, the local shear test, the propensity coarse-graining, the thermal relaxation detection, and the exchange events, which includes Refs. [43,44].
- [43] M. L. Falk and J. S. Langer, *Phys. Rev. E* **57**, 7192 (1998).
- [44] A. Lemaître and C. Caroli, *Phys. Rev. E* **76**, 036104 (2007).
- [45] H. Shiba, Y. Yamada, T. Kawasaki, and K. Kim, *Phys. Rev. Lett.* **117**, 245701 (2016).
- [46] Y. Nishikawa, M. Ozawa, A. Ikeda, P. Chaudhuri, and L. Berthier, *Phys. Rev. X* **12**, 021001 (2022).
- [47] A. Tanguy, F. Leonforte, and J.-L. Barrat, *Eur. Phys. J. E* **20**, 355 (2006).
- [48] C. E. Maloney and A. Lemaître, *Phys. Rev. E* **74**, 016118 (2006).
- [49] C. E. Maloney and A. Lemaître, *Phys. Rev. Lett.* **93**, 195501 (2004).
- [50] H. Kallel, N. Mousseau, and F. Schiettekatte, *Phys. Rev. Lett.* **105**, 045503 (2010).
- [51] G. Kapteijns, D. Richard, and E. Lerner, *Phys. Rev. E* **101**, 032130 (2020).
- [52] L. Berthier, *Phys. Rev. Lett.* **127**, 088002 (2021).
- [53] R. N. Chacko, F. P. Landes, G. Biroli, O. Dauchot, A. J. Liu, and D. R. Reichman, *Phys. Rev. Lett.* **127**, 048002 (2021).
- [54] M. R. Hasyim and K. K. Mandadapu, *J. Chem. Phys.* **155**, 044504 (2021).
- [55] C. Scalliet, B. Guiselin, and L. Berthier, *J. Chem. Phys.* **155**, 064505 (2021).